Table 1. Patient population.

Case	Mat[a] age, years	Gravida[b]	Para[c]	EGA, weeks	Indication	Amnio or CVS	Karyotype	Copies/mL β-actin	Copies/mL SRY	Fetal DNA, %
1	36	4	3	17.1	AMA	Amnio	46,XY	1140	22.6	1.98
2	38	3	0	15.8	AMA	Amnio	46,XY	2990	38.4	1.28
3	34	1	0	15.2	AMA	Amino	46,XY	860	40.1	4.66
4	35	2	1	15.4	AMA	Amnio	46,XX	680	0.0	
5	39	2	1	19.8	AFP+	Amnio	46,XX	640	0.0	
6	34	3	1	9.8	PA	CVS	46,XX	1190	0.0	
7	39	4	1	18.0	AFP+	Amnio	46,XY	1390	96.5	6.94
8	35	2	1	15.4	AMA	Amnio	46,XY	990	69.7	7.04
9	32	2	0	16.0	AFP+	Amnio	46,XX	840	0.0	
10	37	4	0	20.0	AMA	Amnio	47,XY,+21	880	256.5	29.15
11	40	2	1	11.3	AMA	CVS	46,XX	560	0.0	
12	29	1	0	29.3	U/S	Amnio	46,XY	1190	231.1	19.42
13	42	2	1	15.0	AMA	Amnio	46,XY	610	290.9	47.69
14	40	1	0	11.2	AMA	CVS	46,XY	930	94.4	10.15
15	39	3	1	11.2	AMA	CVS	46,XY	660	38.5	5.83
16	32	6	3	19.1	AFP+	Amnio	46,XY	760	125.5	16.51
17	38	1	0	16.1	AMA	Amnio	46,XX	490	0.0	
18	37	13	9	19.3	AFP+	Amnio	46,XX	880	0.0	
19	30	4	2	19.9	AFP+	Amnio	46,XY	670	81.2	12.12
20	34	2	0	17.6	AMA	Amnio	46,XY	510	91.1	17.86
21	23	2	1	23.4	U/S	Amnio	46,XY	510	57.4	11.25
22	39	3	1	15.0	AMA	Amnio	46,XX	940	0.0	
23	39	3	1	16.7	AMA	Amnio	46,XY	490	100.0	20.41
24	41	4	2	17.5	AMA	Amnio	46,XX	1080	0.0	
25	36	3	2	16.5	AMA	Amnio	46,XY	410	13.8	3.37
26	21	1	0	21.5	AFP+	Amnio	46,XX	400	0.0	
27	42	1	0	10.9	AMA	CVS	46,XY	880	103.6	11.77
28	37	3	2	17.1	AMA	Amnio	46,XX	500	0	
29	34	3	2	17.5	AFP+	Amnio	46,XY	830	189.1	22.78
30	30	6	3	19.0	AFP+	Amnio	46,XY	1260	164.5	13.06
Mean								872	111	
SD								474	78	

[a] Mat, maternal; EGA, estimated gestational age; AMA, advanced maternal age (≥35 years at due date); AFP, α-fetoprotein; PA, previous aneuploid pregnancy (i.e., abnormal number of chromosomes); U/S, ultrasound.

[b] Number of pregnancies.

[c] Number of times delivered baby of ≥20 weeks.

This work was supported by the Corporate Office of Science and Technology, Johnson & Johnson, New Brunswick, NJ.

References

1. Bianchi DW, Flint AF, Pizzimenti MF, Knoll JH, Latt SA. Isolation of fetal DNA from nucleated erythrocytes in maternal blood. Proc Natl Acad Sci U S A 1990;87:3279–83.
2. Lo YMD, Corbetta N, Chamberlain PF, Rai V, Sargent IL, Redman CWG, Wainscoat JS. Presence of fetal DNA in maternal plasma and serum. Lancet 1997;350:485–7.
3. Lo YMD, Tein MSC, Lau TK, Haines CJ, Leung TN, Poon PMK, et al. Quantitative analysis of fetal DNA in maternal plasma and serum: implications for noninvasive prenatal diagnosis. Am J Hum Genet 1998;62:768–75.
4. Livak KJ, Flood SJA, Marmaro J, Giusti W, Deetz K. Oligonucleotides with fluorescent dyes at opposite end provide a quenched probe system useful for detecting PCR product and nucleic acid hybridization. PCR Methods Appl 1995;4:357–62.
5. Lo YMD, Lau TK, Zhang J, Leung TN, Chang AMZ, Hjelm NM, et al. Increased fetal DNA concentrations in the plasma of pregnant women carrying fetuses with trisomy 21. Clin Chem 1999;45:1747–51.

Iterative Model for the Calculation of Oxyhemoglobin, Methemoglobin, and Bilirubin in Absorbance Spectra of Cerebrospinal Fluid, *Hendrik J. Duiser, Freek W.C. Roelandse,* Eef G.W.M. Lentjes, Jenny van Loon, John H.M. Souverijn, and Augueste Sturk* (Department of Clinical Chemistry, Leiden University Medical Centre, Albinusdreef 2, 2333 ZA Leiden, The Netherlands; * author for correspondence: fax 31-71-5266753, e-mail froelandse@lumc.nl)

The measurement of the blood pigments oxyhemoglobin, methemoglobin, and bilirubin in cerebrospinal fluid (CSF) has been useful in the differential diagnosis of various hemorrhagic and traumatic disorders of the brain *(1–9)*. Computed tomography often is used for the detection of a hemorrhage, although small vascular bleedings can remain undetectable, in which case the

measurement of blood pigments in CSF might be helpful *(4, 6, 7)*. Detection and quantification of the blood pigments from the absorbance spectra are, however, difficult, and attempts to quantify these pigments *(1, 10, 11)* were not very successful because of factors such as turbidity, pH variability *(11)*, and the large overlap of the absorbance curves, especially those of oxyhemoglobin and methemoglobin *(1, 2, 12)*. The results of the visual interpretation of the spectra are qualitative in nature and depend strongly on the experience of the technicians; results, therefore, are prone to large inter- and intraindividual variation. Our aim was to develop a standardized method for the spectrophotometric examination of CSF and to obtain reliable quantitative results.

A solution to this problem was found in the mathematical step-by-step (iterative) unraveling of the main absorbance scan into the scans of the individual blood pigments via the iterative process.

On arrival at the laboratory, the CSF samples were centrifuged for 10 min at 1800*g* and ambient temperature. The supernatants were kept in the dark to avoid degradation of bilirubin or were stored at −20 °C. Before analysis, the pH of each supernatant was adjusted to pH 6.6 *(11)*. Absorbance scans were then made from 350 to 500 nm on a Beckman DU 640 spectrophotometer. The absorbances at 360, 405, 414, and 455 nm were recorded separately (see Fig. 1, A and B).

Concentrations of the blood pigments were then calculated with a mathematical approximation technique (iteration procedure). In these calculations (see below), the absorbances at 405, 414, and 455 nm, which are the λ_{max} of methemoglobin, oxyhemoglobin, and bilirubin, respectively, were each corrected for the absorbance of the other components. For this we used the relative absorbances of these components at the three wavelengths and the turbidity at 360 nm. The relative absorbance of component *x* is defined as the ratio of the absorbance of a blood pigment *x* at wavelength *y* ($A_{y,x}$) and the maximum absorbance at wavelength λ_{max} ($A_{max,x}$). We determined the relative absorbances at 360, 405, 414, and 455 nm by measuring solutions of pure methemoglobin, oxyhemoglobin, and bilirubin, prepared according to the method of Stroes and van Rijn *(11)*; we used Intralipid (Pharmacia & Upjohn) solutions for turbidity measurements. The absorbance at 360 nm was used as a measure of interference by turbidity. In addition, the measured absorbances were also corrected for a blank CSF sample for which we used fixed absorbance values: 0.011, 0.008, 0.007, and 0.005 absorbance units at 360, 405, 414, and 455 nm, respectively. Repeating the iterative process 20 times appeared to be sufficient in all cases.

For the calculation of, e.g., methemoglobin (m) in the first iteration, the corrected absorbance (A_m) was calculated using the formula:

$$A_{m,n} = A_{405} - (A_{t,n-1} \times t_{405}) - (A_{o,n-1} \times o_{405}) - (A_{b,n-1} \times b_{405})$$

where A_{405} is the absorbance at 405 nm, n is the iteration number (1–20), and o_{405} is the relative absorbance of oxyhemoglobin at 405 nm. The same line of reasoning was used for the other pigments [bilirubin (b), oxyhemoglobin (o), and turbidity (t)]. The recalculated absorbances for the individual pigments were then transformed to concentrations using calibration curves. An example of the original scan of a CSF sample is provided in Fig. 1A. The absorbances contributed by the individual compounds, as calculated by the iterative process, are presented in Fig. 1B.

The linearity of the method was investigated by increasing the concentration of one of the blood pigments in a solution containing high concentrations (3 μmol/L) of the other two pigments. In each case, when the calculated concentration was plotted against the expected concentration, we found a straight line with a slope close to 1 and an intercept that was nearly zero. The lower detection limits calculated from these lines were <0.1 μmol/L for all three pigments.

The reliability of the iterative calculation method was tested with several mixtures of the four components in blank CSF. The results of the added and calculated concentrations in 15 mixtures are presented in Fig. 1C. A close correlation was observed. In addition, we supplemented 27 blank CSF samples with one or more of the blood pigments. Concentrations were calculated with the computer program, and eight experienced technicians interpreted the scans. The results are presented in Table 1, with the presence or absence of an added component used as the "gold standard" to calculate positive and negative predictive values, sensitivities, and specificities. Again, the program calculated the concentrations of the pigments correctly, although two results near the cutoff point of 0.1 μmol/L were discrepant. Nevertheless, the results show that the performance of the computer program is substantially better than the visual interpretation by technicians.

In another approach, using this computer program as the gold standard, 39 absorbance spectra of pathological and nonpathological CSF samples were visually examined by eight trained technicians. The calculated sensitivities [mean (range)] for methemoglobin, oxyhemoglobin, and bilirubin were 0.66 (0.35–1.00), 0.84 (0.54–1.00), and 0.83 (0.67–0.97), respectively. The specificities [mean (range)] were 0.79 (0.37–0.95), 0.42 (0.31–0.54), and 0.88 (0.67–1.00), respectively. There was a large variation in the results between the technicians, which can be overcome by use of the iterative procedure.

In summary, in this study we developed a simple, objective, quantitative, and technician-independent method for the interpretation of CSF spectra. The results show that interpretation of the spectra by individual techni-

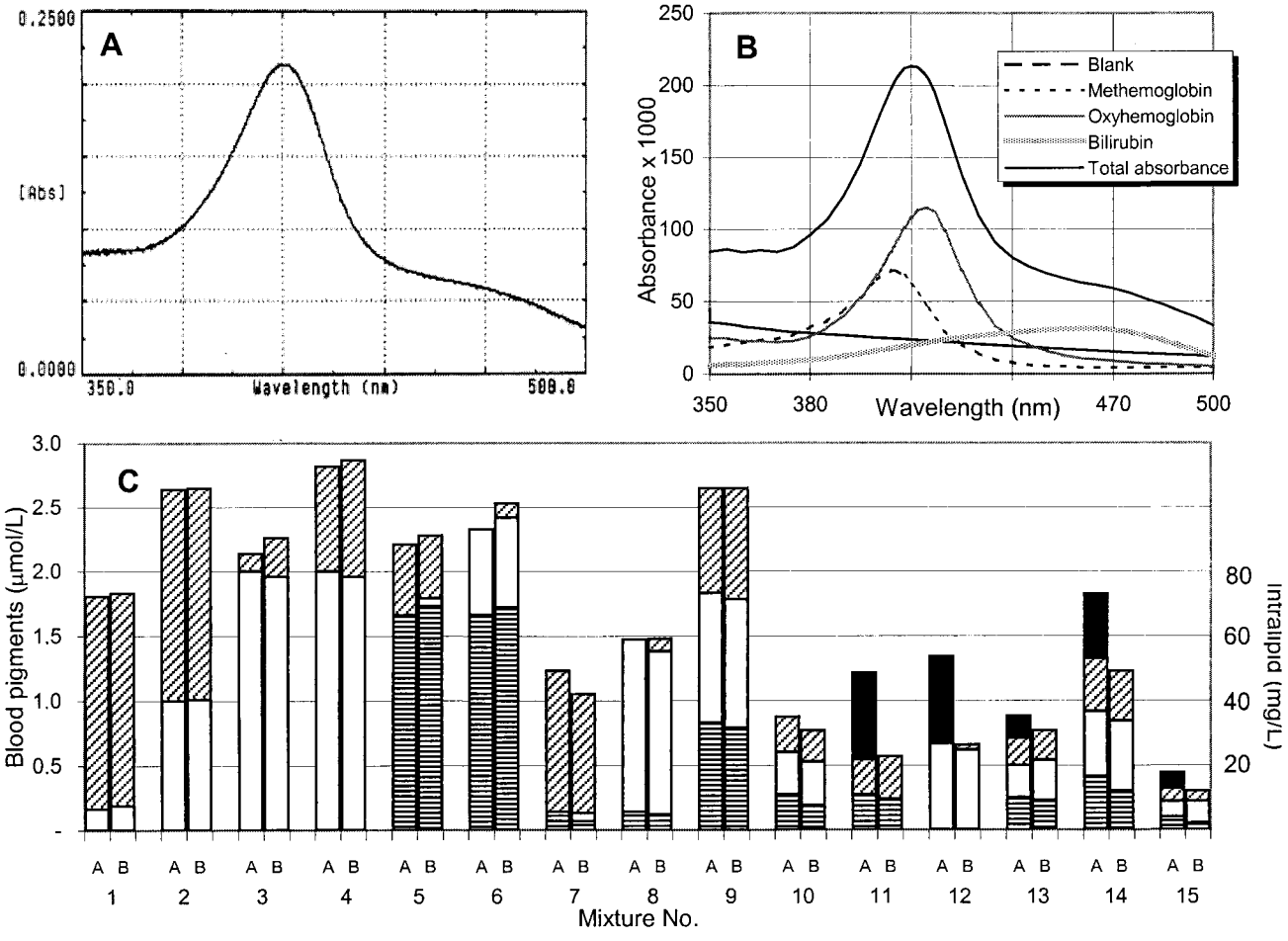

Fig. 1. Application of the iterative method.

(*A*), original absorbance curve of a CSF sample. (*B*), calculated absorbance curves of the individual pigments as calculated by the iterative method. (*C*), comparison of the added (*column A*) and measured (*column B*) concentrations of methemoglobin (▨), oxyhemoglobin (□), and bilirubin (▤) in 15 mixtures of various compositions. Samples 1–10 did not contain Intralipid (■). The final Intralipid concentrations in samples 11–15 were 27, 27, 7, 20, and 5 mg/L, respectively. The concentrations of the three blood pigments are indicated on the *left y-axis* and that of Intralipid on the *right y-axis*.

cians is subject to large intra- and interindividual variation, which complicates a useful clinical interpretation. Our calculation method bypasses these difficulties. However, even if the method is reliable, the results of CSF spectrophotometry must be interpreted carefully by the clinician because blood pigments can appear in CSF without any relation to a hemorrhage *(2, 5–7, 10)*.

We thank the technicians for their assistance. A protected copy of the Microsoft Excel 97 calculation program and a full-size article can be obtained by e-mail free of charge.

Table 1. Comparison of the results from the proposed method with the mean results from eight technicians.[a]

	Methemoglobin (n = 27)				Oxyhemoglobin (n = 27)				Bilirubin (n = 27)			
		Technicians (n = 8)				Technicians (n = 8)				Technicians (n = 8)		
Parameter	Method	Mean	SD	Range	Method	Mean	SD	Range	Method	Mean	SD	Range
Sensitivity	1.00	0.78	0.14	0.61–1.00	1.00	0.82	0.19	0.60–1.00	0.93	0.41	0.27	0.00–0.70
Specificity	0.89	0.74	0.13	0.56–0.90	1.00	0.66	0.13	0.40–0.86	1.00	0.89	0.11	0.67–0.70
PPV[b]	0.95	0.85	0.05	0.76–0.90	1.00	0.87	0.05	0.80–0.92	1.00	0.82	0.32	0.00–1.00
NPV	1.00	0.62	0.17	0.50–1.00	1.00	0.56	0.27	0.30–1.00	0.92	0.92	0.10	0.42–0.70

[a] All 27 CSF samples were supplemented with one or more of the blood pigments.

[b] PPV, positive predictive value; NPV, negative predictive value.

References

1. Kronholm V, Lintrup J. Spectrophotometric investigation of the cerebrospinal fluid in the near-ultraviolet region. Acta Psychiatr Neurol Scand 1960;35: 314–29.
2. Buruma OJS, Janson HLF, van den Bergh FAJTM, Bots GTAM. Blood stained cerebrospinal fluid: traumatic puncture or haemorrhage? J Neurol Neurosurg Psychiatr 1981;44:144–7.
3. Vermeulen M, Gijn van J, Bleijenberg BG. Spectrophotometric analysis of CSF after subarachnoid haemorrhage: limitations in the diagnosis of rebleeding. Neurology 1983;33:112–4.
4. Tsementzis SA, Hitchcock ER, DeCothi A, Gill JS. Comparative studies of the diagnostic value of cerebrospinal fluid spectrophotometry and computed tomographic scanning in subarachnoid haemorrhage. Neurosurgery 1985; 17:908–12.
5. Wahlgren NG, Lindquist C. Haem derivatives in the cerebrospinal fluid after intercranial haemorrhage. Eur Neurol 1987;26:216–21.
6. Trbojevic-Cepe M, Vogrinc Z, Brinar V. Diagnostic significance of methemoglobin determination in colorless cerebrospinal fluid. Clin Chem 1992;38: 1404–8.
7. Page KB, Howell SJ, Smith CML, Dabbs DJW, Malia RG, Porter NR, et al. Bilirubin, ferritin, D-dimers and erythrophages in the cerebrospinal fluid of patients with suspected subarachnoid haemorrhage but negative computed tomography scans. J Clin Pathol 1994;47:986–9.
8. Beetham R, Fahie-Wilson MN, Park D. What is the role of CSF spectrophotometry in the diagnosis of subarachnoid haemorrhage? Ann Clin Biochem 1998;35:1–4.
9. Chalmers AH, Kiley M. Detection of xanthochromia in cerebrospinal fluid. Clin Chem 1998;44:1740–2.
10. Wahlgren NG, Bergström K. Determination of haem derivatives in the cerebrospinal fluid—a semi-quantitative method. J Neurol Neurosurg Psychiatr 1983;46:653–8.
11. Stroes JW, van Rijn HJM. Quantitative measurement of blood pigments in cerebrospinal fluid by derivative spectrophotometry. Ann Clin Biochem 1987;24:189–97.
12. Müller FAJ, Farago F, Kaufmann H, Bürgi W. Methode und klinische bedeutung der liquorspectrophotometrie. Nervenarzt 1989;60:255–61.

Tyrosol Bioavailability in Humans after Ingestion of Virgin Olive Oil, *Elisabet Miró Casas,[1] Magí Farré Albadalejo,[1] Maria Isabel Covas Planells,[2] Montserrat Fitó Colomer,[2] Rosa M. Lamuela Raventós,[3] and Rafael de la Torre Fornell[1*]* [[1] Unitat de Farmacologia, Institut Municipal d'Investigació Mèdica (IMIM) and Universitat Autónoma de Barcelona, Carrer Doctor Aiguader 80, 08003 Barcelona, Spain; [2] Unitat de Lípids i Epidemiologia Cardiovascular, Institut Municipal d'Investigació Mèdica (IMIM), Carrer Doctor Aiguader 80, 08003 Barcelona, Spain; [3] Departament de Bromatologia i Nutrició, Facultat de Farmàcia, Universitat de Barcelona, 08028 Barcelona, Spain; * address correspondence to this author at: Unitat de Farmacologia, Institut Municipal d'Investigació Mèdica (IMIM), Carrer Doctor Aiguader 80, 08003 Barcelona, Spain; fax 34-932213237, e-mail rtorre@imim.es]

Results from epidemiological studies support the relationship between the consumption of phenolic-rich food and a low incidence of coronary heart disease *(1, 2)*. The lower incidences of coronary heart disease and certain cancers in Mediterranean countries have been associated with diet, of which fruits, vegetables, legumes, and grains are the usual components and the major fat component is olive oil *(3)*. The Mediterranean dietary pattern has been also shown to be effective in secondary prevention of coronary heart disease *(4)*. Virgin olive oil is rich in phenolic compounds with strong antioxidant properties that protect olive oil from autooxidation *(5)*. In addition, olive oil phenolic compounds have been shown to delay in vitro metal-induced and radical-dependent LDL oxidation *(6, 7)*. Among the phenolic compounds in olive oil is tyrosol (4-hydroxyphenylethanol), which is also present in other dietary sources *(8, 9)* and has mild antioxidant properties *(10–12)*. However, information on the bioavailability of dietary phenolic compounds in humans is scarce *(13, 14)*. In bioavailability studies of phenolic compounds, one of the main problems is the estimation of the dose administered because these substances can be present in multiple forms in food. In the specific case of olive oil, phenolic compounds may be in the form of glycosides, polymers, and esters *(12, 15)*. To our knowledge, the bioavailability of tyrosol from nonsupplemented dietary sources has not been described previously.

Eight healthy volunteers were recruited (five men and three women; age range, 25–52 years). The local ethics committee, CEIC-IMAS (register no. 98/798/I), approved the protocol, and participants signed an informed consent. All volunteers could be considered healthy on the basis of physical examination and standard biochemical and hematological tests. Subjects had an mean weight of 75 ± 13.47 kg (men, 83.2 ± 4.4 kg; women, 59.7 ± 6.11 kg) and a body mass index of 25.6 ± 3.1 kg/m^2 (men, 26.9 ± 3.29 kg/m^2; women, 22.4 ± 2.4 kg/m^2). Volunteers followed a phenolic-free diet for 4 days (wash-out period) before acute olive oil administration. A nutritionist designed dietary recommendations and diet during the 24-h experimental period. Volunteers were instructed to exclude several foods from their diet (coffee, tea, fruits, vegetables, wine, and olive oil). At 0800 on day 5, they were provided with 50 mL of extra virgin olive that was administered in a single dose ingested either directly (n = 2) or with some bread (n = 6). Olive oil was the sole phenolic dietary source in the next 24 h. Urine was collected before the start of the wash-out period (pre-wash-out period; first voided spot urine in the morning), during the wash-out period (first voided spot urine in the morning), and after the acute administration period (at 0–4, 4–8, 8–12, 12–16, and 16–24 h) and stored at −80 °C until analysis.

The tyrosol content in virgin olive oil usually is evaluated after extraction with methanolic water without other sample treatment *(16)*. This method permits only the determination of free tyrosol in olive oil. In this bioavailability study, aliquots of methanolic water extracts of the olive oil administered were submitted to either an acidic or an alkaline treatment. This was done to release tyrosol from its conjugated form and to experimentally reproduce some of the gastrointestinal conditions occurring during digestion of oil in humans. Sample preparation was performed using a modification of a method previously described by Caruso et al. *(12)*. A 15-mL aliquot of the olive oil administered in the study was extracted three times with methanol-water (80:20 by volume). Pooled extracts were treated with hydrochloric acid (1 mol/L HCl; sample pH adjusted to 1) or sodium hydroxide (0.1 mol/L NaOH; sample pH adjusted to 10) with further sonication (30 min at 45 kHz) at room temperature. After 60 min of incubation, the methanolic water extracts were evaporated under reduced pressure at 40 °C on a rotary evaporator (Rotavapor RE 121; Büchi). Aqueous